Supplementary Material

Effect of Nitrogen Dopant Agents in the Performance of Graphene-Based Cathodes for Li-S Batteries

Adrián Licari, Almudena Benítez *, Juan Luis Gómez-Cámer, Rafael Trócoli and Álvaro Caballero *

Dpto. Química Inorgánica e Ingeniería Química, Instituto Químico para la Energía y el Medioambiente (IQUEMA), Facultad de Ciencias, Universidad de Córdoba, 14071, Córdoba, Spain.
* Correspondence: q62betoa@uco.es (A.B.); alvaro.caballero@uco.es (Á.C.);
Tel.: +34-957218621 (A.B.); +34-957218620 (Á.C.)

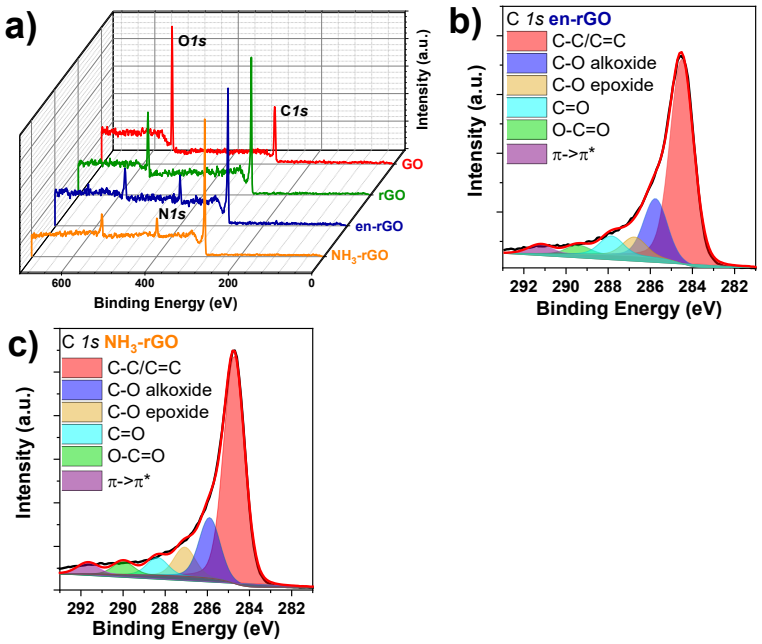

Figure S1. a) XPS survey for the GO, rGO, en-rGO and NH_3-rGO samples; XPS spectrum of the C*1s* signal for the b) en-GO, and c) NH_3-rGO samples.

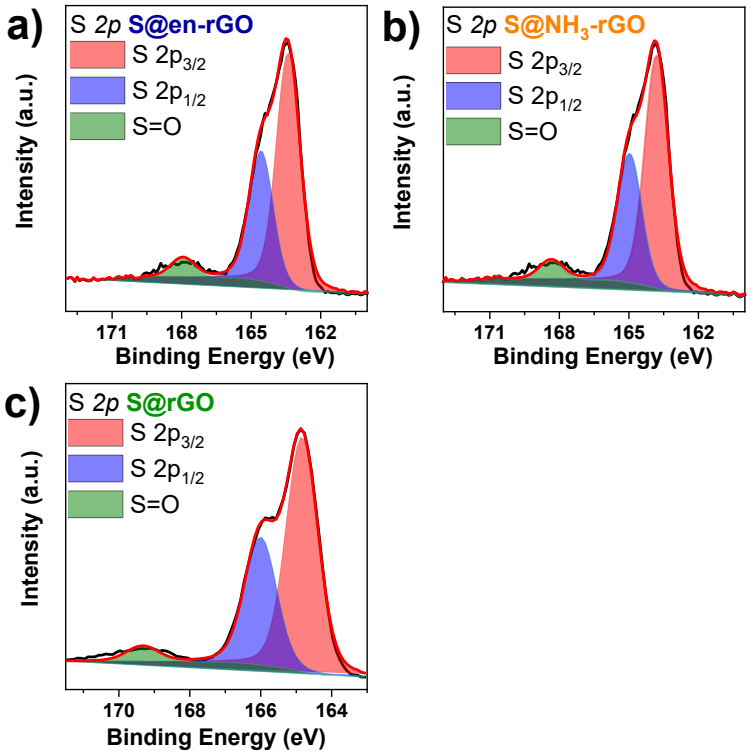

Figure S2. XPS spectrum of the S *2p* signal for the a) S@en-GO, b) S@NH_3-rGO, and c) S@rGO samples.

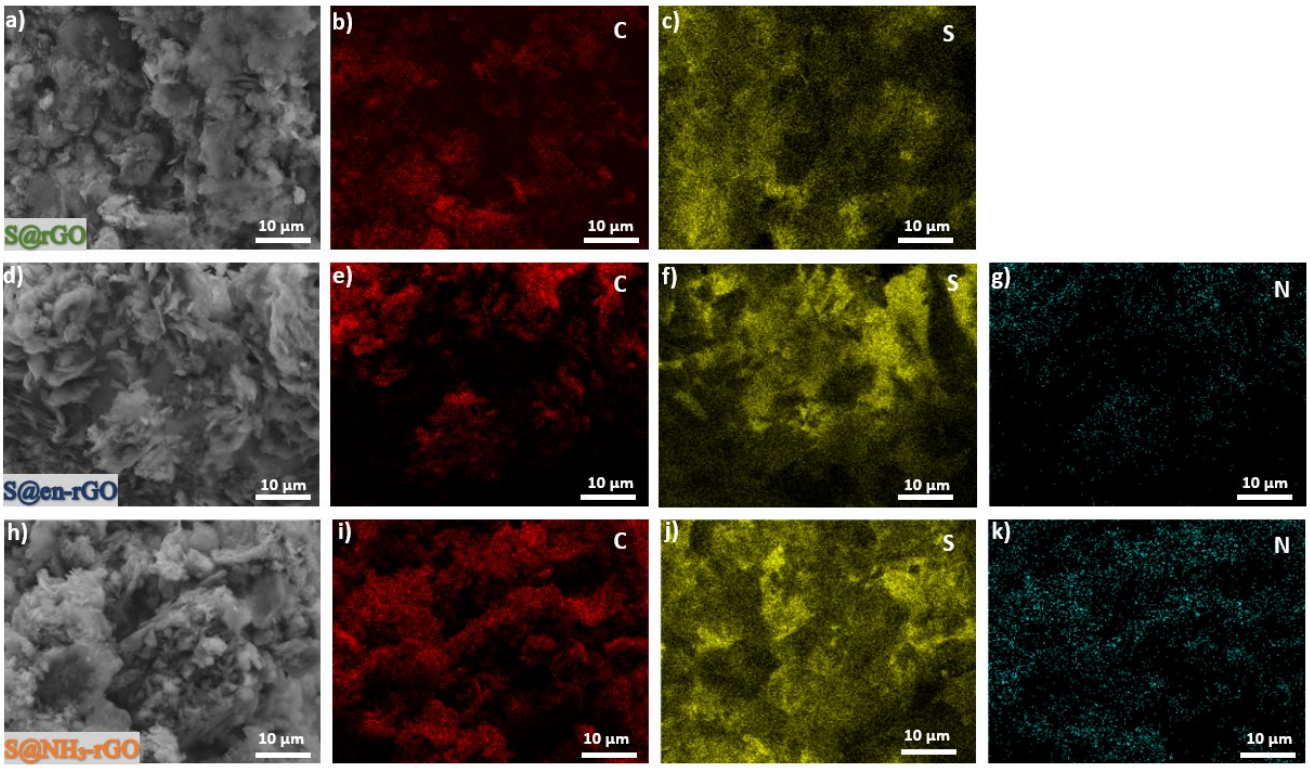

Figure S3. SEM images of the a) S@rGO, d) S@en-GO and h) S@NH_3-rGO samples; EDX analysis of the S@rGO sample: b) carbon and c) sulfur; S@en-GO sample: e) carbon, f) sulfur and g) nitrogen: and S@NH_3-rGO sample: i) carbon, j) sulfur and k) nitrogen.

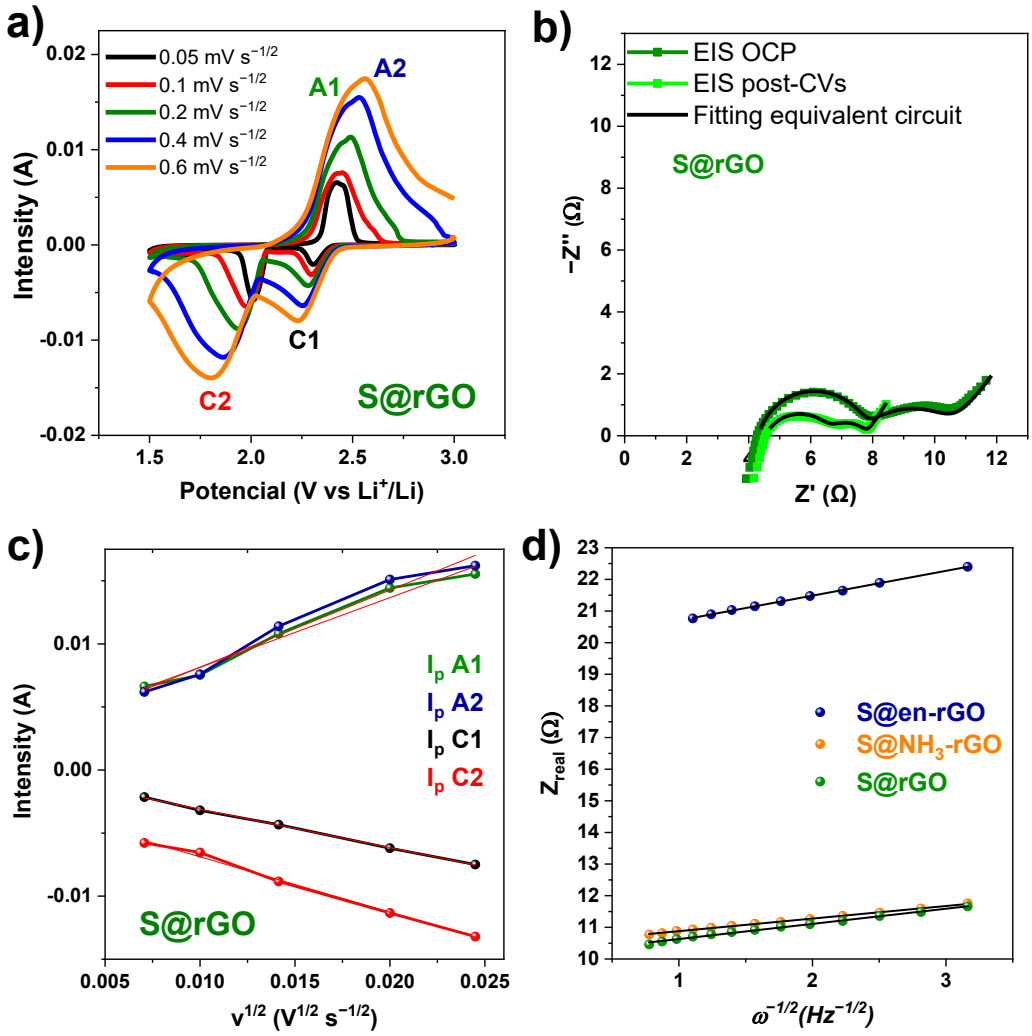

Figure S4. a) Cycle voltammograms at 0.05, 0.1, 0.2, 0.4 and 0.6 mV s^{-1} between 3.0 and 1.5 V for the S@rGO electrode; b) Impedance spectra for S@rGO electrode; c) Graphical representation of peak intensity versus sweep speed elevated to a half for the S@rGO electrode; and d) Graphical representation of real impedance component (Z_{real}) versus $\omega^{-1/2}$ in the Warburg region to evaluate the σ term for equation (2) for the S@en-GO, S@NH_3-rGO and S@rGO electrodes.

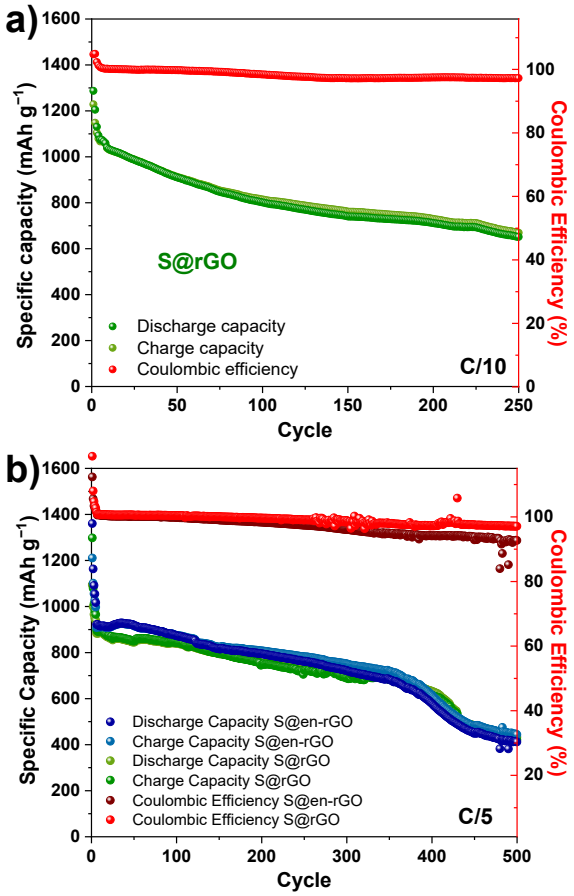

Figure S5. a) Long-term discharge/charge capacity values as a function of the cycle number and the coulombic efficiency at C/10 rate for the S@rGO electrode; b) Long-term discharge/charge capacity values as a function of the cycle number and the coulombic efficiency at C/5 rate for S@en-rGO and S@rGO electrodes.

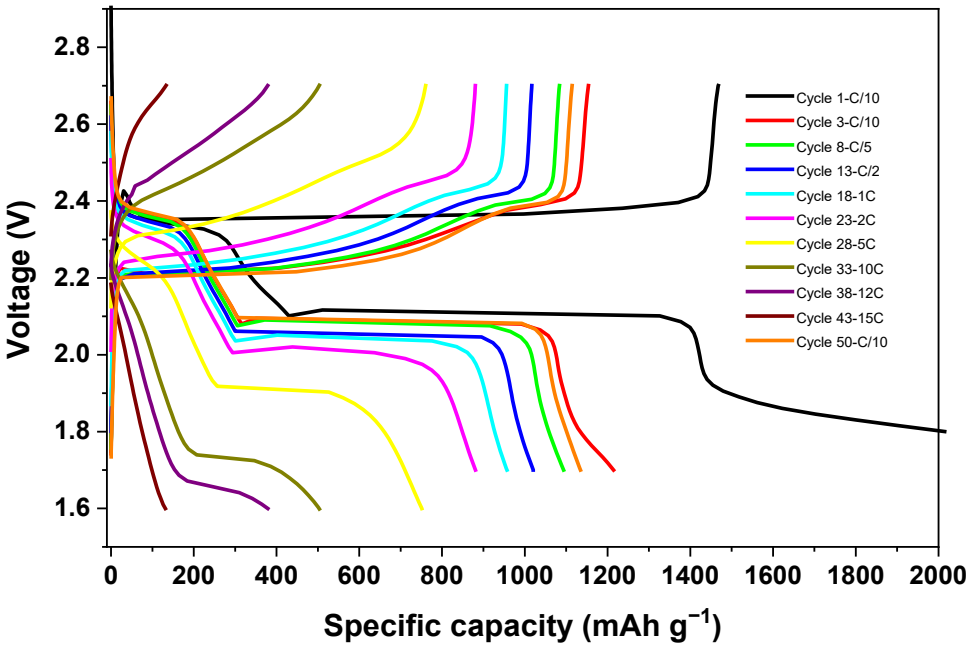

Figure S6. Charge/discharge profiles at C/10, C/5, C/2, 1C, 2C, 5C, 10C, 12C, and 15C rates of the Li-S cells with the$S@NH_3$-rGO electrode.

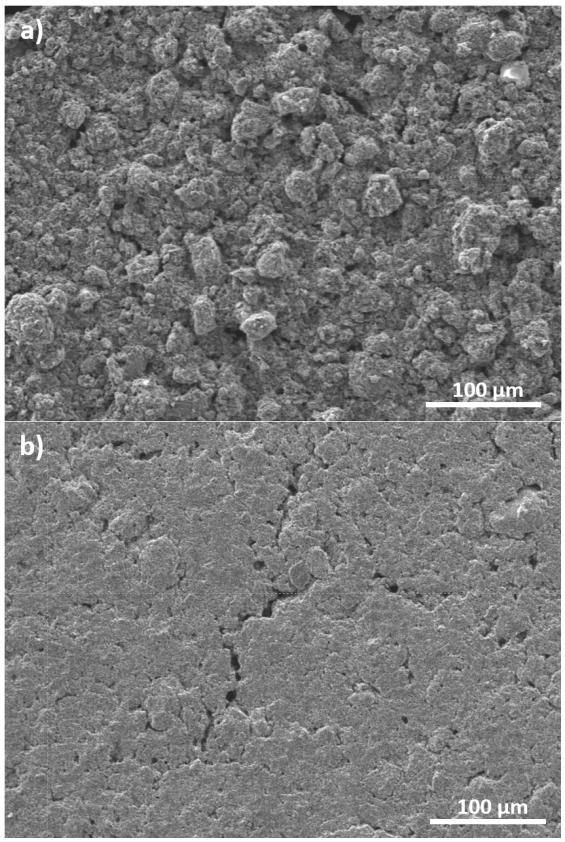

Figure S7. SEM images of the NH_3-rGO electrode (a) before and (b) after rate capability test (C/10, C/8, C/5, C/3, C/2, 1C and 2C; 5 cycles each and C/10 again during 50 more cycles).

Table S1. Values of the impedances' components, χ^2, τ and Li^+ ion diffusion coefficients ($cm^2\ s^{-1}$) of the S@en-rGO, S@NH_3-rGO and S@rGO electrodes obtained by applying the equation (2).

Samples	EIS	χ^2	R_e (Ω)	R_{int} (Ω)	R_{ct} (Ω)	τ_{ct} (s)	σ ($\Omega \cdot s^{-1/2}$)	D_{EIS}
S@en-rGO	OCP	$2.80 \cdot 10^{-4}$	5.42	11.49	3.86	0.014	0.78	$2.05 \cdot 10^{-9}$
	Post-CV	$4.90 \cdot 10^{-4}$	4.65	2.41	3.57			
S@NH_3-rGO	OCP	$1.20 \cdot 10^{-3}$	4.51	3.52	2.94	0.004	0.40	$7.96 \cdot 10^{-9}$
	Post-CV	$1.48 \cdot 10^{-3}$	3.48	2.36	0.94			
S@rGO	OCP	$1.10 \cdot 10^{-3}$	4.33	3.40	2.97	0.008	0.48	$5.49 \cdot 10^{-9}$
	Post-CV	$1.27 \cdot 10^{-3}$	4.54	2.08	1.20			

Table S2. Li^+ ion diffusion coefficients ($cm^2\ s^{-1}$) of the S@en-rGO, S@NH_3-rGO and S@rGO electrodes obtained by applying the Randles-Sevcik equation (1).

	S@en-rGO	S@NH_3-rGO	S@rGO
A1	0.60	0.62	0.55
A2	0.64	0.68	0.61
C1	-0.29	-0.34	-0.31
C2	-0.40	-0.50	-0.44
D_{Li} (A1)	$2.89 \cdot 10^{-6}$	$3.10 \cdot 10^{-6}$	$2.43 \cdot 10^{-6}$
D_{Li} (A2)	$3.27 \cdot 10^{-6}$	$3.69 \cdot 10^{-6}$	$2.97 \cdot 10^{-6}$
D_{Li} (C1)	$6.59 \cdot 10^{-7}$	$9.34 \cdot 10^{-7}$	$7.40 \cdot 10^{-7}$
D_{Li} (C2)	$1.29 \cdot 10^{-6}$	$2.02 \cdot 10^{-6}$	$1.53 \cdot 10^{-6}$